Chemical Engineering Journal 146 (2009) 249–258

Contents lists available at ScienceDirect

Chemical Engineering Journal

journal homepage: www.elsevier.com/locate/cej

High temperature sequestration of CO_2 using lithium zirconates

Alina Iwan[a], Hazel Stephenson[b], William C. Ketchie[c], Alexei A. Lapkin[a,*]

[a] Catalysis and Reaction Engineering Group, Department of Chemical Engineering, University of Bath, Bath BA2 7AY, UK
[b] MEL Chemicals, PO Box 6, Lumns Lane, Swinton, Manchester M27 8LS, UK
[c] UOP LLC, 50 E. Algonquin Road, Des Plaines, IL 60017, USA

ARTICLE INFO

Article history:
Received 18 September 2007
Received in revised form 26 May 2008
Accepted 9 June 2008

Keywords:
Carbon dioxide sequestration
Lithium zirconate
Sorption enhanced reforming

ABSTRACT

Equilibrium and kinetics of CO_2 reaction with lithium zirconates synthesised by two different methods are reported. Considerably faster rates of high temperature reaction were obtained for the new material synthesised by a soft-chemistry route without the use of alkaline metal dopants, in comparison with the available literature data, with the highest rate 0.83 wt% min^{-1}. Lithium zirconate was found to be stable in consecutive forward–backward reaction cycles. Reaction rate dependency on the partial CO_2 pressure was examined. The apparent slow reaction rates at $p_{CO_2} < 0.4$ bar are due to mass transfer limitations. Detailed analysis of the reverse reaction of decomposition of lithium carbonate–zirconia mixed matrix revealed complex three-step behaviour, which was associated with the transition from reaction to mass transfer control. The latter was successfully eliminated in the material prepared from a high surface area zirconia precursor. Low temperature interaction between lithium zirconate and CO_2 revealed during experiments performed at 25–550 °C is also discussed.

1. Introduction

Separation of CO_2 is a significant industrial challenge in a number of areas from enhanced oil recovery, to control of breathing atmosphere in enclosed spaces, reduction in green house gases emissions of power plants or shift of thermodynamic equilibrium of large scale reactions such as steam reforming. In all these applications the function of CO_2 separation is not the primary objective. It is considered as additional 'cost' to the main process and, therefore, comes with rather strict economic/performance constraints on the viability of application of any new materials in the carbon dioxide recovery process. This issue has recently been discussed in the literature [1,2]. The main performance criteria are the sorption capacity, the rate of sorption/reaction, the rate of regeneration and the lifetime of the scavenging solution or a solid material.

Amongst the many potential applications of CO_2 sorbents or membranes, the process of lower temperature steam reforming – the sorption enhanced reforming process (SERP) [3–6] – presents particularly severe materials performance constraints due to the temperatures at which the CO_2 capture should occur (450–600 °C), the need for very high rates of sorption/regeneration and the long-term material stability. A review of inorganic materials potentially suitable for high temperature sorption of CO_2 identified hydrotalcites as the most promising class of materials, possessing both a reasonable sorption capacity (0.3–0.5 mmol g^{-1} at 400 °C) and a sufficiently fast rate of sorption [7]. Besides hydrotalcites, which have been extensively studied for the potential applications in high temperature CO_2 recovery [8–10], other materials attracting significant interest are basic metal oxides obtained from naturally abundant minerals such as dolomite [11,12], and synthetic reactive capture agents, such as lithium zirconate [13–16] and lithium silicate [17–19].

The latter class of materials offers selective capture of carbon dioxide, based on the formation of solid carbonates, as shown in Eq. (1) for the case of lithium zirconate, and high capacity of sorption, *e.g.*, up to 28.75% of CO_2 by weight stoichiometric uptake onto lithium zirconate. The forward reaction occurs in the temperature range of 450–550 °C and the reversible reaction of decomposition of lithium carbonate and the formation of lithium zirconate is starting above 650 °C [13,20]. The high temperature of decomposition of the carbonates is a major drawback of all mineral CO_2 scavengers, due to a very high energy demand of the regeneration process.

$$Li_2ZrO_{3(s)} + CO_{2(g)} \overset{450\,^\circ C<T<650\,^\circ C}{\underset{T>650\,^\circ C}{\rightleftharpoons}} Li_2CO_{3(s)} + ZrO_{2(s)} \quad (1)$$

The second well-documented drawback of the mineral CO_2 capture materials is the slow reaction rate, which is associated with the formation of diffusional barrier towards CO_2, as explained previously via the core–shell or the dual core–shell reaction mechanisms [20,21].

* Corresponding author. Tel.: +44 1225 383360; fax: +44 1225 385713.
E-mail address: A.Lapkin@bath.ac.uk (A.A. Lapkin).

1385-8947/$ – see front matter © 2008 Elsevier B.V. All rights reserved.
doi:10.1016/j.cej.2008.06.006

The rate of CO_2 mass transfer can be effectively improved by establishing an eutectic mixture of alkaline carbonates with a minimum of melting point below the process temperature of sorption, via doping the starting lithium zirconate material with, *e.g.*, stoichiometric amount of potassium carbonate [22]. Diffusion of CO_2 through the molten carbonate is much faster than in the solid lithium carbonate, which results in a faster rate of reaction. The acceleration effect was found to be even greater in the case of tertiary carbonates, *i.e.* using lithium, potassium and sodium carbonates [21]. As the presence of molten carbonate was proven to be critical for the faster rate of reaction, many combinations of carbonates were tested at different temperatures [23,24].

A further improvement in the reaction rate can be achieved by decreasing the particle size, thus decreasing the diffusional length [14,23,25]. Recently published results by Ochoa-Fernandez et al. [26] show a significant increase in the reaction rate using tetragonal nano-crystalline undoped lithium zirconate prepared by a soft-chemistry method. However, the method of preparation shown in Ref. [26] involves an explosive step, which severely limits the scale of production of lithium zirconates via this route.

In this paper we describe recent results on detailed characterisation of lithium zirconate materials prepared by a traditional solid state synthesis and a new soft-chemistry route, by which small seed crystallites are produced, whilst the gentle calcination procedure results in the materials with a high specific surface area. The new method does not involve combustion of an organic template and is readily scaleable. The obtained materials are characterised by a considerably faster rate of reaction compared to the data available in the open literature. The detailed study of reaction with CO_2 as a function of temperature revealed significant uptake at low temperatures, which may potentially open new applications for the lithium zirconates in the medium-temperature CO_2 sequestration processes, such as carbon capture in power stations. The paper presents detailed thermodynamic and mechanistic analysis of the low-temperature interaction of CO_2 with lithium zirconates. We have also investigated the dependence of reaction rate on CO_2 partial pressure, identifying significant mass transfer limitation at partial pressures below 400 mbar.

2. Experimental

2.1. Materials

Lithium zirconate samples of various compositions were synthesised by MEL Chemicals. Lithium zirconates were obtained following the widely described method of mixing a zirconia precursor with lithium carbonate, followed by calcination to invoke the reverse reaction shown in Eq. (1) [13,20,27]. The main difference with the earlier described methods, is the use of zirconium hydroxide rather than zirconium oxide at the stage of mixing with lithium carbonate. This permits a much closer mixing of the reactants in the aqueous slurry phase, as opposed to solid state mixing employed in the traditional synthesis, and permits lower calcination temperatures (700–775 °C) preventing the collapse of the surface area.

Sample A (Melsorb 1596/01): target composition 91.3 wt% Li_2ZrO_3, 3.4 wt% Y_2O_3, 0.2 wt% Al_2O_3, 5.1 wt% K_2O. The sample was prepared by slurrying a zirconium hydroxide doped with 5.3 wt% Y_2O_3 and 0.25 wt% Al_2O_3 having a d_{50} of ~15 μm, in deionised water. Lithium carbonate was added slowly followed by potassium carbonate, and the resultant mixture was stirred for 30 min prior to calcination at 775 °C for 4 h in static air using ramp rate 3 °C min^{-1}.

Sample B (Melsorb 1596/02): target composition 91.5 wt% Li_2ZrO_3, 3.4 wt% Y_2O_3 and 5.1 wt% K_2O. The sample was prepared in the same way as sample A except the d_{50} of Y_2O_3-doped zirconium hydroxide was ~1 μm.

Sample C (Melsorb 1597/03): Li_2ZrO_3 was prepared in the same way as samples A and B, but the zirconium hydroxide used was prepared by a novel preparation method which gives it high surface area, larger pore size and a higher pore volume, than the hydroxides used in samples A and B.

The particle size of the hydroxide precursors is carefully controlled during the preparation. Details on the soft-chemistry route are given in the patent application [28].

A reference sample for comparison was obtained from Aldrich. A list of samples is given in Table 1. Gases CO_2 (99.8%) and N_2 (99.99%) used in all experiments were obtained from BOC.

2.2. Characterisation methods

Images were obtained with a JEOL 6310 scanning electron microscope (SEM) instrument using gold-coated samples. Specific surface area (BET) and pore volume were measured using low temperature nitrogen sorption on a Tristar 3000 instrument following degassing at 180 °C over 3 h. Particle size of lithium zirconate precursors was measured using a Microtrac X100 instrument. The XRD patterns were collected on a Bruker D8 Advanced Diffractometer, with Cu Kα radiation over the range of 15–65° 2θ. Samples were initially pre-treated under nitrogen at 750 °C for 2 h. XRD patterns were then recorded in a synthetic air mixture or CO_2 at specific temperatures, stabilising the temperature for 30 min.

2.3. CO_2 reaction experiments and thermal stability

Samples A and B were treated at 750 °C in the flow of nitrogen for 16 h and sample C for 2 h prior to measurements of CO_2 uptake to eliminate carbon dioxide captured from air during transportation or storage of the materials. Thermal stability of samples and uptake of CO_2 in the flow experiments at *ca.* 1 bar CO_2 pressure were studied using a Setaram TG-92 instrument. Temperature programmed reaction was carried out in the CO_2 or N_2 flow, in the case of reversible reaction, *ca.* 28 mL (STP) min^{-1}, with the rate of temperature increase 1 °C min^{-1}. Long-term stability was studied over five consecutive experiments at 500 °C in the CO_2 flow. Between each cycle the sample was regenerated at 750 °C in the N_2 flow.

Experiments at low pressures of CO_2 were performed using an Intelligent Gravimetric Analyser (IGA, Hiden). Sample, placed in a platinum wire basket inside the stainless steel chamber, was evacuated over 10 h at 490–495 °C. Reaction was carried out over a pressure range of 5–1000 mbar at 490–495 °C, with 1–3 h equilibration time at each set pressure point. Dynamics of mass change was recorded at each pressure point, with temporal resolution of *ca.* 5 s.

3. Results and discussion

3.1. Structural characterisation of lithium zirconate samples

SEM images of the lithium zirconate samples synthesised by MEL Chemicals are shown in Fig. 1. Samples A and B were prepared using a starting zirconia species with the seed particle sizes of approximately 1 and 15 μm, respectively, measured by light scattering of aqueous dispersed samples. Calcination of the zirconia precursor with the lithium species produces materials consisting of agglomerates of bound particles. Based on the analysis of SEM images, the agglomerates in sample A are loose and built up from the seed particles of 0.2–1.3 μm diameter. In sample B the agglomerates appear to be considerably more fused, producing particles of 8–15 μm, whereas spherical seed particles could be identified

Table 1
Composition and structural data of the lithium zirconate samples

	Units	Melsorb 1596/01 (sample A)	Melsorb 1596/02 (sample B)	Melsorb 1597/03 (sample C)	Aldrich
Surface area (BET)	$m^2\,g^{-1}$	1.56	0.49	10.87	0.48
Total pore volume	$cm^3\,g^{-1}$	0.004	0.003	0.030	0.001
Y_2O_3	wt%	3.4	3.4	0	0
K:Zr	mole ratio	0.2:1.0	0.2:1.0	0	0
Li:Zr	mole ratio	1.1:1.0	1.1:1.0	1.1:1.0	Unknown

with the particle sizes between 0.7 and 4 μm. The material also contains other phase, which is believed to be the potassium carbonate promoter. Presence of K and Al was confirmed by EDX analysis during SEM measurements, as expected from the starting composition. The microscopy data show discrepancy with the light scattering. However, the general trend is confirmed: sample B consists of agglomerates of considerably larger seed particles, which should result in a lower specific surface area. Based on the low temperature nitrogen sorption data, sample B has three times lower BET surface area and a slightly lower pore volume (see Table 1) which corresponds well with the larger size of the seed particles and apparently denser agglomerates, as evidenced by microscopy.

Sample C was made using an alternative starting zirconia species, with a primary particle size of approximately 4 μm. This material was designed to have a significantly improved stability of pore structure than that used to make samples A and B. This should translate into a higher surface area and pore volume of the resultant lithium zirconate. A ~1 μm zirconium hydroxide prepared by the same process as that for samples A and B calcined at 700 °C for 2 h will have a total pore volume of 0.15 mL g^{-1}, whereas the zirconium hydroxide used to make sample C when calcined at 700 °C for 2 h has a total pore volume of 0.27 mL g^{-1}.

An SEM image of sample C, see Fig. 1C, shows that primary particles have open porous structure, markedly different from these of samples A and B. It is possible to identify primary particles of *ca.* 5 μm in diameter, which are clearly highly porous. Based on the nitrogen sorption data the surface area and pore volume of sample C are an order of magnitude higher than these for the earlier materials (see Table 1).

Diffraction patterns of samples were recorded using in situ method either in a synthetic air ($O_2 + N_2$ mixture) or in CO_2. Fig. 2 shows the patterns recorded from sample A. The initial pattern was collected on the sample 'as-received', prior to treatment in nitrogen. There is a marked difference with the sample recorded following the initial treatment in the inert atmosphere: reflection at 30°, assigned to Li_2CO_3, disappears and all reflections corresponding to lithium zirconate increase in magnitude. Similarly, reflections that are assigned to ZrO_2 are present in the 'as-received' sample, which may be due to (i) incomplete conversion during the initial preparation or (ii) the low-temperature reaction with atmospheric carbon dioxide.

Upon increase in temperature in the synthetic air atmosphere reflections do not change, thus confirming thermal stability of the synthesised lithium zirconate. The observed pattern is best fit to the reference tetragonal lithium zirconate pattern [29]; no lithium carbonate reflections were observed in the sample following the initial thermal treatment in nitrogen. Minor reflection around 30° is likely to correspond to K_2CO_3, which was added as promoter at the synthesis stage. The presence of potassium was confirmed by X-ray analysis during SEM measurements. Small reflections at 20° could be assigned to a minor presence of monoclinic lithium zirconate phase. These reflections also disappear in the presence of CO_2 at high temperature, thus confirming that they belong to lithium zirconate.

Upon an increase in temperature in the presence of CO_2 (see Fig. 2), the characteristic reflections of Li_2ZrO_3 at 22, 23, 36, 40, 42, 60 and 62° 2θ disappear, whereas reflections of zirconia (marked with asterisks) and of Li_2CO_3 (at 30°) appear, thus confirming the formation of zirconia and lithium carbonate. The reaction is effectively complete at 650 °C.

The patterns shown in Fig. 3 were recorded with sample C in the atmosphere of CO_2. The 'as-received' sample is also shown for comparison. The low temperature patterns are similar to these of sample A: the pattern effectively corresponds to tetragonal lithium zirconate phase, although a higher presence of monoclinic phase is evident; see Fig. 4 for comparison between samples. The 'as-received' sample shows much stronger reflections of zirconia and carbonates than the corresponding pattern for sample A. No carbonates or zirconia reflections were observed following the thermal treatment in nitrogen, since any carbonate would have been removed by the treatment at 750 °C. Reaction with CO_2 commences above 450 °C. The pattern recorded after 1 h exposure to CO_2 at 650 °C shows stronger reflections of monoclinic zirconia (see reference spectra [30]), than the equivalent pattern for sample A in

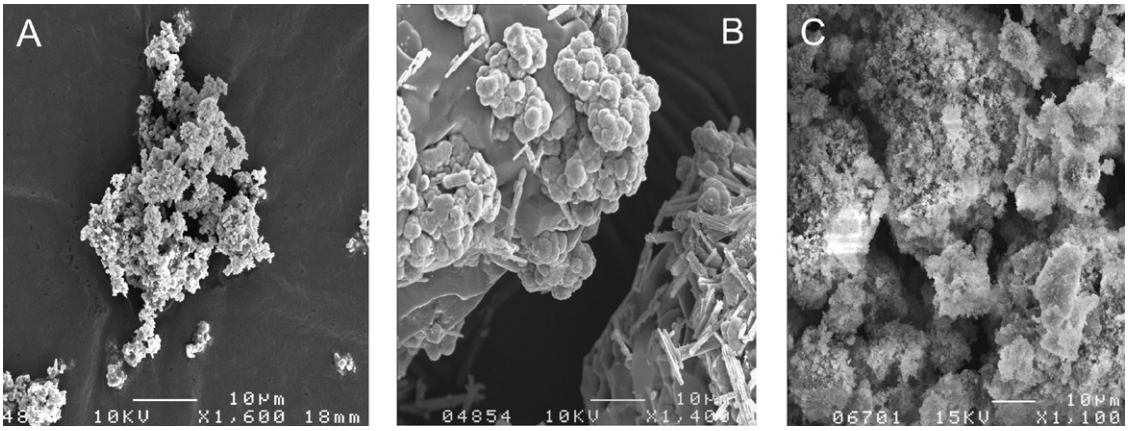

Fig. 1. SEM images of lithium zirconate samples: fine (A) and coarse (B) samples from the same zirconia precursor, and the sample (C) prepared from a new zirconia precursor.

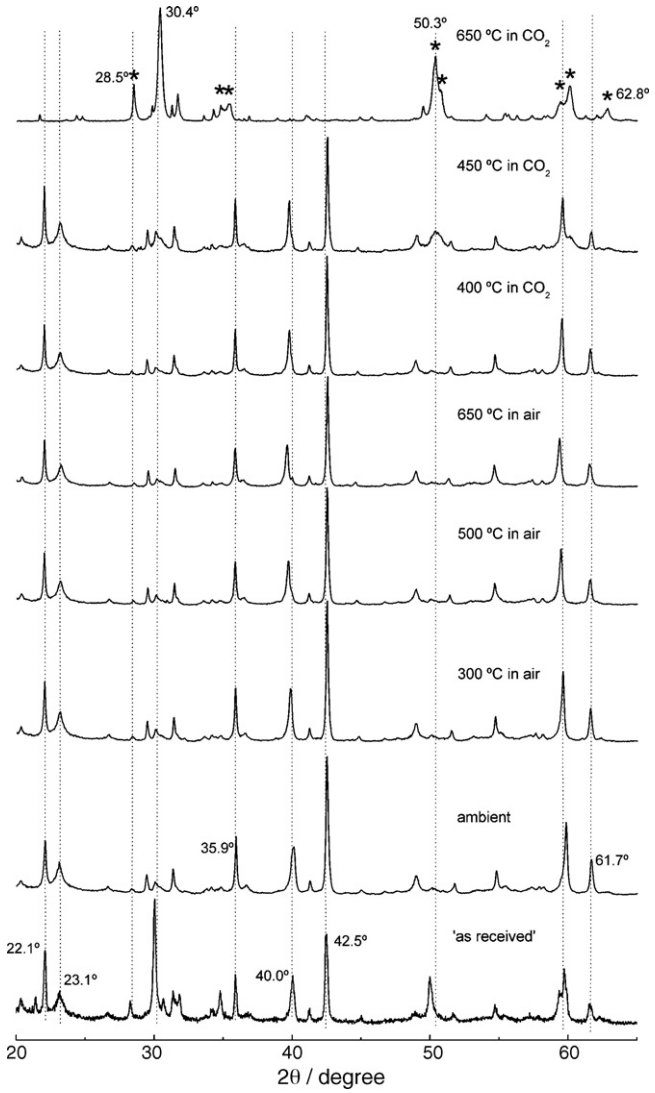

Fig. 2. In situ powder diffraction patterns of sample A, measured in synthetic air and in CO_2 at different temperatures. "*" indicate reflections corresponding to ZrO_2.

Fig. 2. Also, more minor reflections are identifiable in this pattern, most belonging to lithium and potassium carbonates.

Reflections of the reference sample of lithium zirconate purchased from Sigma–Aldrich are shown in Fig. 4 along with the reflections collected from samples A and C after the initial thermal treatment. The marked differences in the patterns is likely to be due to higher fraction of monoclinic lithium zirconate in the Sigma sample, in comparison with the Melsorb samples, which contain preferentially tetragonal phase. It is also evident that sample C contains a higher amount of monoclinic phase, in comparison to sample A.

The XRD data of 'as-received' samples (see Figs. 2 and 3) show the presence of lithium carbonate and zirconia that might have formed on the sampled during, *e.g.*, transportation or storage exposed to ambient air. Detailed gravimetric analysis of the 'as-received' samples confirms the presence of carbonates. Fig. 5 shows mass loss during thermal treatment of samples in the flow of nitrogen. The initial mass loss at temperatures below 100 °C corresponds to drying, whereas further loss at temperatures above 500 °C is attributed to the loss of carbon dioxide upon decomposition of carbonates. The presence of carbonates in the 'as-received' samples can be associated either with the incomplete reaction during initial preparation, or with the uptake of CO_2 from atmosphere upon transport of samples.

3.2. Thermodynamic analysis

Based on the thermodynamic analysis it should be possible to assess the range of temperature and pressure favouring the forward or reversible reactions given by Eq. (1). Results of thermodynamic analysis of reaction of CO_2 with lithium silicate and lithium zirconate at a constant (1 bar) pressure of CO_2 were recently published without describing details of calculations [31]. However, it is useful to present such details, and also to obtain results as a function of pressure, which would reflect the actual process involving the low-pressure regeneration step.

Since the reaction involves both the solid and the gaseous species an expression for Gibbs free energy involves partial pressure

Fig. 3. In situ powder diffraction patterns of sample C measured in CO_2 at different temperatures. "*" indicate reflections corresponding to ZrO_2.

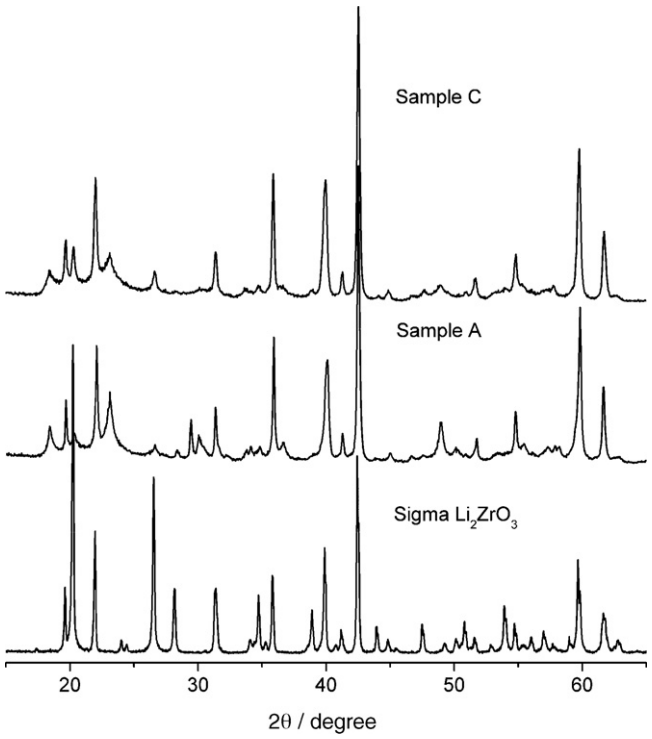

Fig. 4. Comparison of powder diffraction patterns of samples A and C with the standard commercial sample of lithium zirconate sourced from Sigma–Aldrich.

of CO_2:

$$\Delta G = \sum_i \eta_i \Delta H_i - T\sum_i \eta_i \Delta S_i + \eta_{CO_2} RT \ln\left(\frac{p_{CO_2}}{p^0}\right) \quad (2)$$

where η is a stoichiometric coefficient of species i in the reaction shown in Eq. (1), ΔH_i and ΔS_i are the enthalpy and entropy of formation of component i, given as temperature function equations in the following equations, and p^0 is the standard pressure:

$$\Delta H_i = \Delta H^0_{298_i} + A_i t + B_i \frac{t^2}{2} + C_i \frac{t^3}{3} + D_i \frac{t^4}{4} - \frac{E_i}{t} + F_i - H_i \quad (3)$$

$$\Delta S_i = A_i \ln(t) + B_i t + C_i \frac{t^2}{2} + D_i \frac{t^3}{3} - \frac{E_i}{2t^2} + G_i, \quad t = \frac{T}{1000} \quad (4)$$

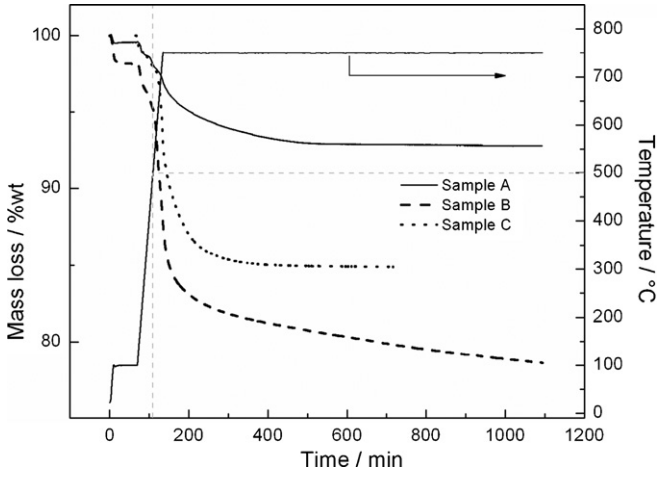

Fig. 5. Thermal stability of the lithium zirconate samples A, B and C (all samples initially 'as-received').

Therefore, it is possible to derive the dependence of Gibbs free energy on pressure, which establishes the condition of spontaneous reaction ($\Delta G < 0$):

$$\sum_i \eta_i \Delta H_i - T\sum_i \eta_i \Delta S_i - RT \ln\left(\frac{p_{CO_2}}{p^0}\right) < 0,$$

$$\frac{p_{CO_2}}{p^0} > \exp\left(\frac{\sum_i \eta_i \Delta H_i}{RT} - \frac{\sum_i \eta_i \Delta S_i}{R}\right) \quad (5)$$

The necessary parameters for the calculation of the Gibbs free energy of reaction for Li_2CO_3, ZrO_2 and CO_2 were published elsewhere [32]. However, the existing data for lithium zirconate [33] does not correspond well with our experimental data. Furthermore, the expression for Gibbs energy of formation of Li_2ZrO_3 presented in the available literature [33] results in the apparently wrong temperature dependence, contradicting to the general behaviour of solids [34]. To overcome this problem we obtained a new temperature dependency for Li_2ZrO_3. The Gibbs energy of formation of Li_2ZrO_3 can be described as a polynomial function of temperature:

$$\Delta G_{Li_2ZrO_3} = \Delta G^0_{298} + aT + bT^2 \quad (6)$$

As a starting point, the values of coefficients a and b were evaluated from the Gibbs energy for lithium silicate [32]. The obtained dependence for the Gibbs energy of reaction as a function of temperature and pressure was then fitted to the experimental data by root mean square method. The fitted coefficients for Eq. (6) are $a = 4.4 \times 10^{-5}$ and $b = 9.311 \times 10^{-2}$.

The final equation for Gibbs energy of reaction of CO_2 with lithium zirconate is given by the following equation:

$$\Delta G_r = \sum_j \eta_j \Delta H^0_{298_j} - \sum_j \eta_j A_j t(\ln(t) - 1) - \frac{t^2}{2}\sum_j \eta_j B_j - \frac{t^3}{6}\sum_j \eta_j C_j - \frac{t^4}{12}\sum_j \eta_j D_j - \frac{1}{2t}\sum_j \eta_j E_j + \sum_j \eta_j F_j - t\sum_j \eta_j G_j - \sum_j \eta_j H_j - \Delta G_{Li_2ZrO_3} + \eta_{CO_2} RT \ln\left(\frac{p_{CO_2}}{p^0}\right) \quad (7)$$

where η is a stoichiometric coefficient of species j, *i.e.* CO_2, Li_2CO_3 and ZrO_2, in the reaction shown in Eq. (1).

Using this expression the temperature–pressure envelope for the forward and the reversible reactions was calculated, shown in Fig. 6. At a partial pressure of CO_2 = 1 bar, the forward reaction of formation of carbonates will take place up to approximately 700 °C. Above this temperature the reversible reaction is thermodynamically more favourable. Theoretically, the reversible reaction can proceed at temperatures as low as 550 °C, by lowering the CO_2 pressure below 10 mbar. It is also clear that the reaction of formation of carbonates can proceed at low temperatures. Therefore, the observed formation of carbonates upon transportation and storage of the lithium zirconate samples agrees with thermodynamics.

3.3. Equilibrium and dynamics of CO_2 reaction with lithium zirconates

Mass uptake of carbon dioxide was measured in the dynamic experiments under temperature ramping conditions (see Fig. 7). The blank test in the nitrogen flow showed no mass change, thus establishing that mass uptake corresponded to the reaction with carbon dioxide only. For all samples a significant mass uptake was registered in the presence of CO_2 at temperatures above 400 °C.

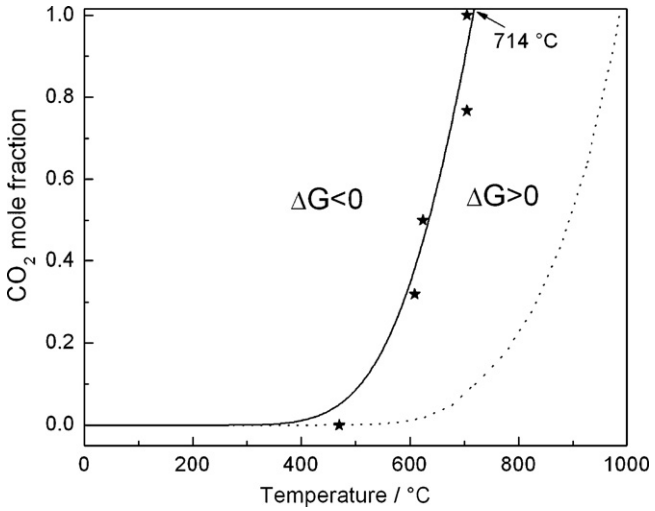

Fig. 6. Dependence of Gibbs free energy of reaction of CO_2 with lithium zirconate as a function of CO_2 gas phase partial pressure and temperature (dotted line, model using lithium silicate thermodynamic data; solid line, model with fitted coefficients for lithium zirconate; stars, experimental data).

A much smaller mass uptake was also observed at temperatures above 150 °C for the MEL samples.

The maximum rates of reaction were calculated from the experimental data and are given in Table 2. Sample C, characterised by the highest surface area, exhibited the highest rate of reaction at the mean temperature of 485 °C. Sample C also exhibited the highest rate of the reversible reaction, which is exhibited as the apparent mass loss at temperature above 720 °C, shown in Fig. 7. The relative change of the rates of the forward and the reversible reactions through the sample series is the same. Notably, there is no apparent correlation between the rates of reactions and the surface areas in samples A and B (see data in Tables 1 and 2). The apparent correlation of the maximum mass uptake and the surface area would be misleading, since the stoichiometric uptake may not have been reached in the "slower" samples under conditions of dynamic experiments.

The rates of reaction were significantly higher for all samples produced by MEL in comparison with that of pure Li_2ZrO_3 obtained from Aldrich. Sample C showed the maximum rate of 0.83 wt% min^{-1} compared with 0.38 for the Aldrich sample, 0.58 for the Toshiba TOS U700 sample [35], or 0.18 for the K-doped lithium silicate (480 °C) [18]. It was suggested that the monoclinic lithium zirconate exhibits slower uptake of CO_2 in comparison with the tetragonal phase [16]. This view is supported by our data, since the comparison of the XRD patterns of the samples, see Fig. 4, reveals a much higher fraction of monoclinic phase in the Aldrich sample, in comparison with the Melsorb samples.

Table 2
The rates of the forward and reversible reactions obtained from the temperature programmed experiments

Material	Maximum rate of forward reaction (wt% min^{-1})	Maximum CO_2 uptake (wt%)	Maximum rate of reversible reaction (wt% min^{-1})
Sample A	0.58 (460–500 °C)	28.34	1.17 at 756 °C
Sample B	0.71 (450–480 °C)	27.26	1.26 at 763 °C
Sample C	0.83 (480–500 °C)	29.87	1.57 at 754 °C
Aldrich	0.38 (520–550 °C)	26.46	0.81 at 738 °C

Temperature ramp, 1 °C min^{-1}; CO_2 flow, *ca.* 27 cm^3 (STP) min^{-1}.

Samples A–C (Fig. 6) showed a marked uptake of CO_2 between 100 and 260 °C. This uptake was not observed for the sample obtained from Aldrich. No further mass gain was observed between 260 and 400 °C. A similar behaviour is clearly seen in the results for lithium zirconates [36] and also for lithium silicates [18] reported in the literature. Sorption of CO_2 at temperatures above 200 °C, with a maximum at *ca.* 350 °C was also reported for Li_2O [37], Na_2ZrO_3 and $Li_{2-x}Na_xZrO_3$ [38].

The possibility of the low-temperature uptake from the point of view of thermodynamics has been shown above (see Fig. 6). In a recent paper the mechanism of low-temperature CO_2 interaction with lithium silicate is attributed to the reaction with Li_2O present in the material, leading to the formation of carbonate [31]. However, it was said that low temperature interaction of CO_2 with lithium zirconate is not feasible due to very slow reaction. The uptake at 200–350 °C on Li_2O and on Na_2ZrO_3 and $Li_{2-x}Na_xZrO_3$ was attributed to the surface reaction with Li, forming surface lithium carbonate layer [37,38]. Because no experiments revealing the energy of interaction between CO_2 and lithium ceramics are reported in the earlier literature, it is impossible to assess the influence of the weaker chemisorption processes over the feasibility of surface reaction. In the case of the suggested mechanism of low temperature CO_2 uptake depending on the presence of surface Li_2O species, it is rather questionable, since the oxide sublimes at 780 °C — the temperature of pre-treatment of our materials,

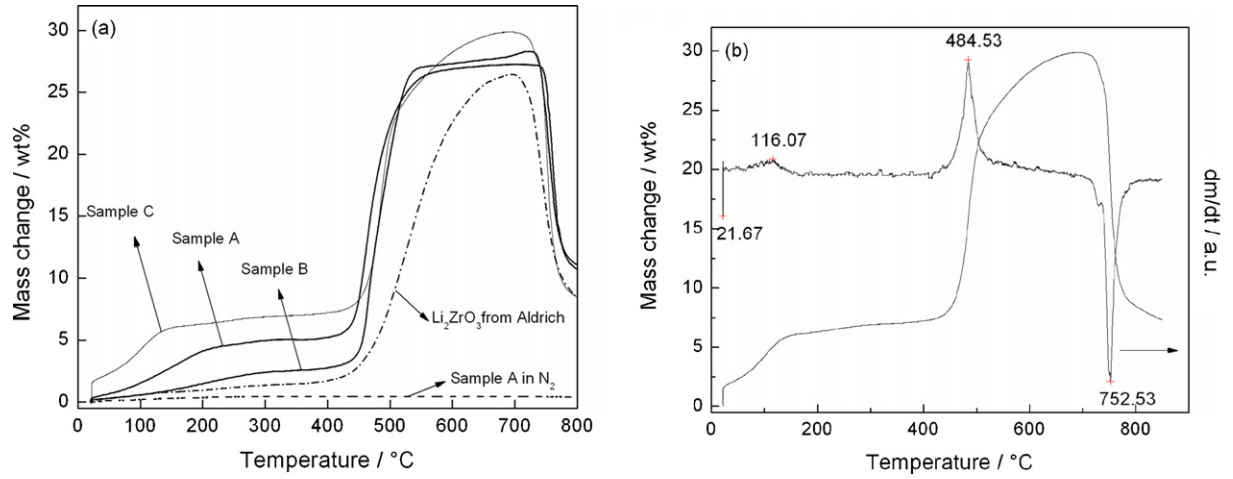

Fig. 7. Reaction of CO_2 with the lithium zirconate samples under conditions of CO_2 flow and temperature ramping. Temperature ramp, 1 °C min^{-1}; CO_2 flow, *ca.* 27 cm^3 (STP) min^{-1}. (a) Mass change data *vs.* temperature; (b) the rate of reaction (dm/dt) with sample C.

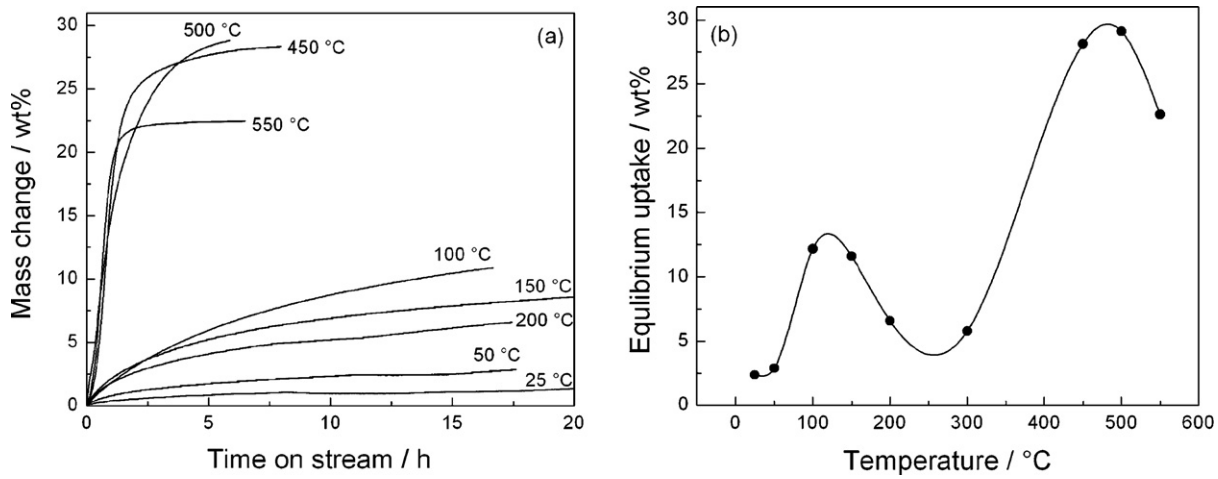

Fig. 8. Isotherms of CO_2 uptake on the lithium zirconate sample A at different temperatures: (a) reaction profile *vs.* time-on-stream and (b) saturation values obtained by extrapolation to infinite time.

after which no oxide could be present on the surface, whilst the phenomenon persists.

To study the low-temperature interaction of CO_2 with lithium zirconates in more detail a series of reactions were performed at different temperatures between 25 and 550 °C and results are shown in Fig. 8. Uptake of CO_2 was observed in all tests, with a fast uptake observed at the temperatures above 450 °C and slow, but significant, uptake at the temperatures below 200 °C. The maximum uptakes calculated by extrapolation of the measured data at each temperature to infinite time plotted against temperature, confirmed the existence of the two distinct temperature regions in which interaction of carbon dioxide and lithium zirconate occurs by different mechanisms (Fig. 8b). The uptake at the higher temperatures, with the maximum at *ca.* 450 °C, is caused by the chemical

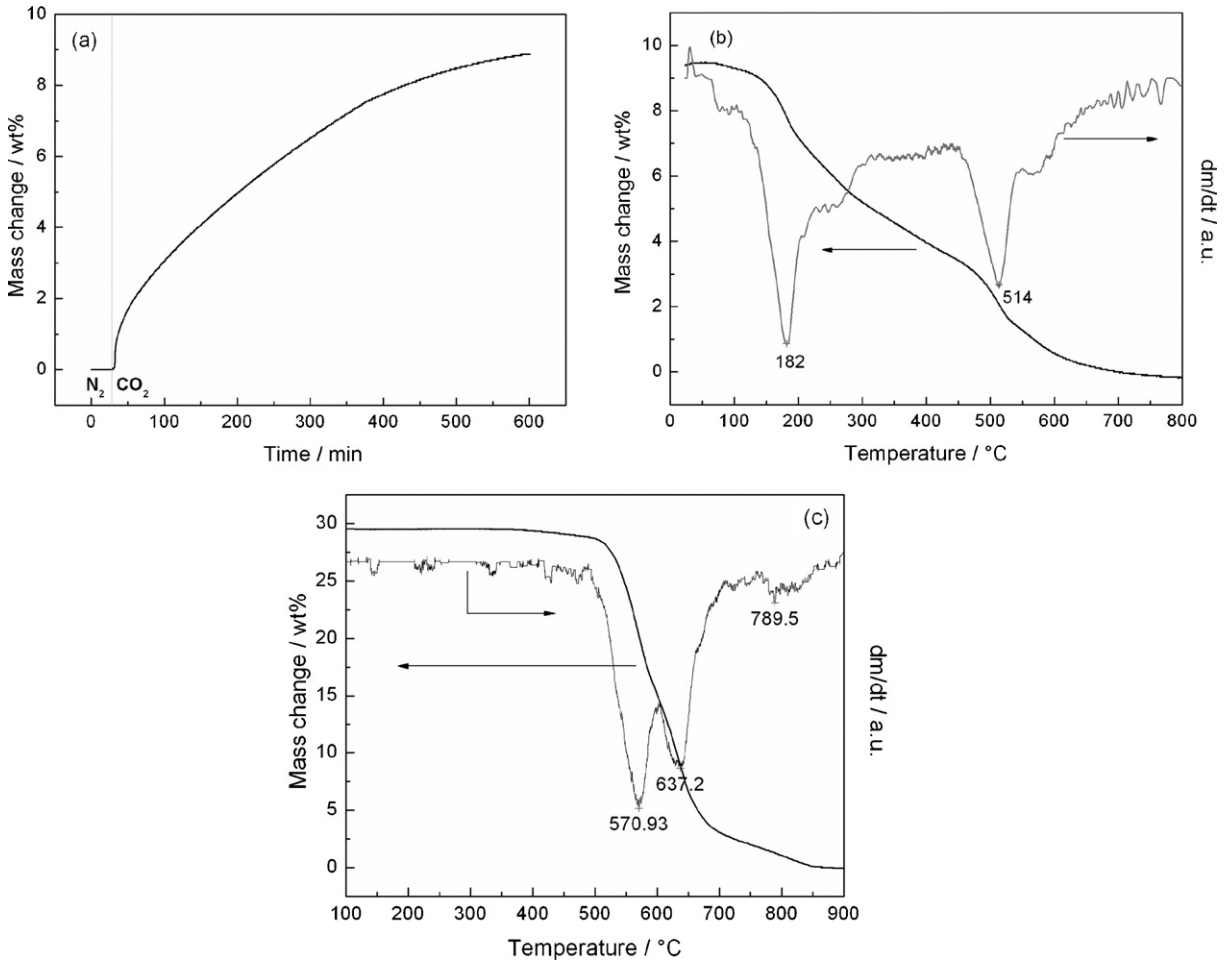

Fig. 9. CO_2 uptake onto sample C at 22.5 °C (a), temperature programmed desorption following the room temperature uptake (b) and high temperature uptake (c).

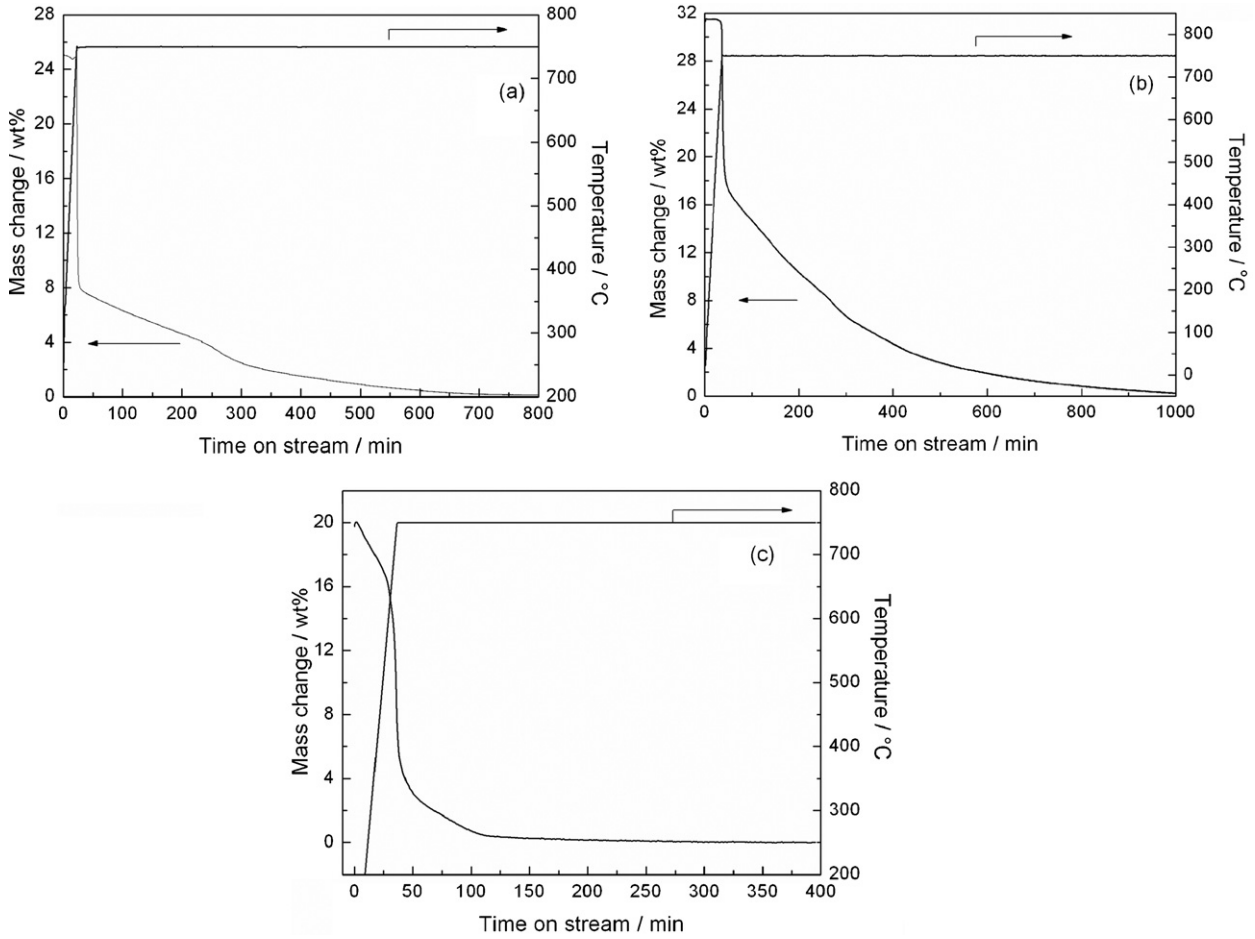

Fig. 10. Reversible decomposition reaction of lithium carbonate at 750 °C of samples A, B and C (a, b and c accordingly). Temperature ramp, 20 °C min^{-1}; N_2 flow, *ca.* 20 mL min^{-1}.

reaction between solid lithium zirconate and gaseous CO_2. It is believed that a different mechanism is responsible for the low temperature uptake (with maximum at *ca.* 125 °C), most likely based on weaker chemisorption interactions.

The existence of the two different mechanisms of interaction of CO_2 with lithium zirconate can be confirmed by a sequence of temperature programmed desorption (TPD) experiments, following (i) sorption/reaction at room temperature and (ii) reaction at temperatures above 260 °C. Results of the former test are shown in Fig. 9. The sample was exposed to CO_2 at about 22 °C for 10 h and then flushed with nitrogen for 1 h to remove the physically adsorbed CO_2. A significant uptake of CO_2 is registered, *ca.* 9 wt%. The TPD profile reveals mass loss at temperatures above 100 °C, with the highest rate at 182 °C (Fig. 9b). It is believed, that this corresponds to the loss of chemisorbed CO_2 from the basic sites. The second peak, observed at 514 °C, corresponds to decomposition of lithium carbonate. Therefore, it is clear that at low temperatures, reaction of carbon dioxide with lithium zirconate does proceed, however, with a much slower rate, and it is accompanied by chemisorption on basic sites present in the material.

The TPD profile of lithium zirconate following the high temperature reaction with carbon dioxide (Fig. 9c) reveals a different behaviour: mass loss is observed only at temperatures above 500 °C, with the highest rate at approximately 570 °C. It is clear that the sites responsible for the low-temperature uptake of CO_2 are not active at elevated temperatures, thus confirming that the low-temperature uptake is in part due to chemisorption and not solely due to the slow chemical reaction.

3.4. Reversible reaction of carbonates decomposition: regeneration of Li_2ZrO_3

Fig. 10 shows mass loss as a function of time for samples A and B at 750 °C in the flow of nitrogen, following reaction with CO_2 at 500 °C. Three distinct rates of mass loss can be observed. In the first few minutes, once the set temperature is reached, decomposition of carbonates proceed rapidly and mass loss of 13.5% for sample A made of the fine precursor particles (Fig. 10a) and 10.6% for sample B made of the coarse precursor particles (Fig. 10b) are reached. In the second step, the rate of mass loss sharply decreases and remains linear for about 250 min in the case of sample A.

Finally, in the third step, the rate of mass loss is very slow and follows an exponential curve, reaching constant mass in about 700 min for sample A and 1000 min for sample B. The shape of mass loss *vs.* time-on-stream curve is less distinct in the case of the material with the coarse structure.

It is believed that the first step of mass loss corresponds to the reaction of carbonates decomposition occurring near the surface of particles and is not mass transfer limited, reflecting the true rate of reaction. The initial rate of decomposition reaction is estimated to be 5.4–6.9 wt% min^{-1}. The consecutive decrease in the rate of mass loss, shown in Fig. 10, corresponds to progressively increasing influence of mass transfer. This hypothesis could be confirmed by

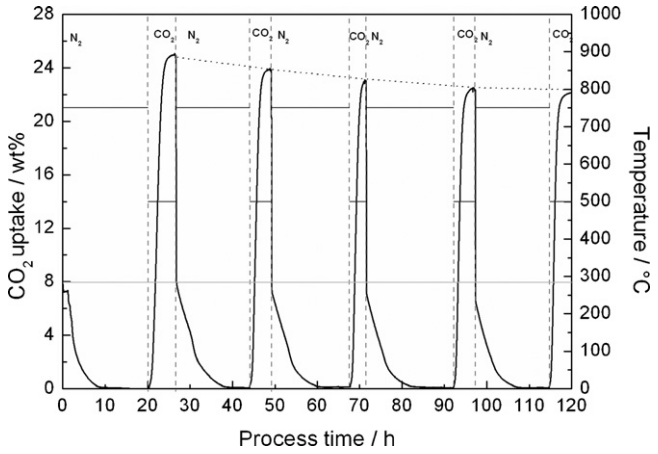

Fig. 11. Stability of lithium zirconate material (sample A) tested in consecutive reaction–regeneration experiments. Reaction carried out in CO_2 flow *ca.* 27 cm^3 (STP) min^{-1} at 500 °C. Regeneration carried out in N_2 flow *ca.* 27 cm^3 (STP) min^{-1} at 750 °C.

the lack of the three-step mass loss *vs.* time-on-stream profile in the case of sample C (see Fig. 10c). For this material the overall time required to complete regeneration is a factor of 2 and 3 shorter than for samples A and B, respectively. Thus, fundamentally, the rate of regeneration of lithium zirconates as CO_2 scavenging materials can be reasonably high. However, this requires high surface area of the seed zirconia material and small size of the seed zirconia crystallites in order to minimise the effects of mass transfer.

3.5. Material stability

Stability of lithium zirconates in cycling reaction–regeneration operation was tested in a series of five consecutive cycles with samples A (Fig. 11) and C (Fig. 12). The first regeneration stage of sample A showed a decrease in the mass of the sample, corresponding to decomposition of remaining lithium carbonate in the as-received sample. High mass uptake of carbon dioxide, close to the maximum stoichiometric uptake, was observed in all cycles. A small degradation in capacity observed over five cycles became progressively less significant. This suggests that after a small number of cycles the operating capacity of the material should become stable and, by extrapolation, would correspond to 85.8% of the stoichiometric amount. The maximum rate of forward reaction was constant in every cycle and calculated to be about 0.43 wt% min^{-1}. The existing data does not allow us to speculate on the exact reason for the stabilisation of material at this particular value of stoichiometric uptake.

In the case of sample C a different stabilisation behaviour was observed, with the material exhibiting a progressively higher maximum uptake of CO_2, equilibrating at *ca.* 25.5 wt% uptake (see Fig. 12). The reason is also likely to be in the detailed structural rearrangement of the particles, which enable better access to lithium carbonate over the course of first three cycles. This demonstrates the benefit of using the starting material with a more open structure, enabling better access to reactants.

There are two main differences between samples A and C, that may contribute to the difference in the samples stabilisation behaviour: (i) sample A was stabilised with yttria and has preferentially tetragonal phase, whereas sample C has a mixture of tetragonal and monoclinic phases, and (ii) sample C has a higher surface area. Both factors may contribute to the stabilisation behaviour. The tetragonal phase could be incompletely regenerated in sample A, whereas re-structuring of sample C through first few cycles could enhance the accessibility of the lithium zirconate for CO_2. Detailed analysis of these factors is currently underway.

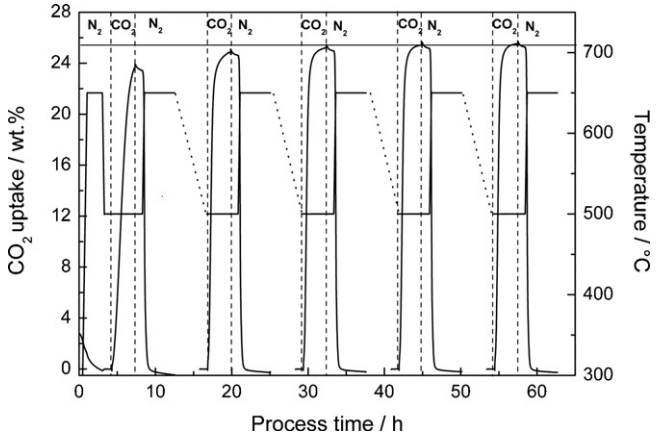

Fig. 12. Stability of lithium zirconate material (sample C) tested in consecutive reaction–regeneration experiments. Reaction carried out in CO_2 flow *ca.* 27 cm^3 (STP) min^{-1} at 500 °C. Regeneration carried out in N_2 flow *ca.* 27 cm^3 (STP) min^{-1} at 750 °C.

3.6. Pressure dependence

It was reported earlier that dynamics of sorption at lower partial CO_2 pressure is significantly reduced [13,22,25], although no explanation was given. Reactions at different partial pressures of CO_2 were performed at 490–494 °C with sample C. Based on the preceding discussion, only reaction is responsible for the uptake of carbon dioxide at this temperature. Therefore, a linear dependence of reaction rate on gas pressure is expected, according to reaction stoichiometry (Eq. (1)). Thus, reaction rate should be directly proportional to CO_2 pressure, with the order of reaction with respect to CO_2 partial pressure equals 1:

$$r = kp_{CO_2}^{n} \tag{8}$$

where r is the rate of reaction, k is the rate constant, p_{CO_2} is partial pressure of carbon dioxide above sample, and n is the order of reaction.

Fig. 13 shows that above 400 mbar of carbon dioxide pressure the apparent rate of reaction is a linear function of pressure. How-

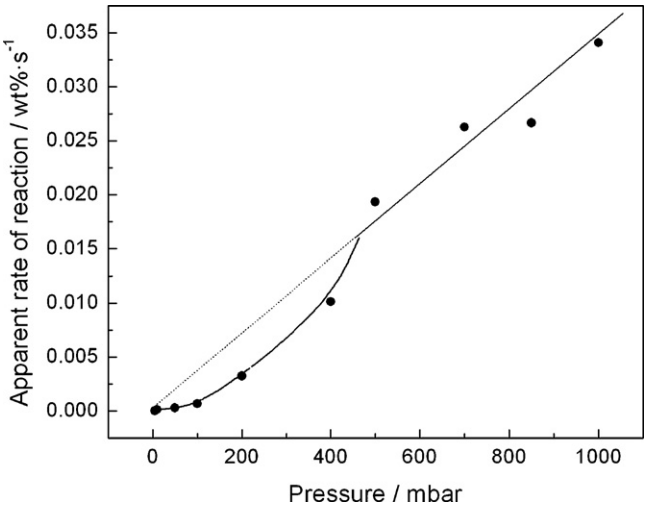

Fig. 13. Relationship between apparent rate of reaction and CO_2 pressure on the lithium zirconate sample C. Reaction carried out at 0–1000 mbar of CO_2 at 490–495 °C, with 1–3 h equilibration time at each point.

ever, below 400 mbar the apparent rate deviates from the linear relationship. An exponential dependence at low pressures indicates diffusion limitations.

4. Conclusions

Two formulations of lithium zirconate CO_2 scavengers were synthesised and characterised. It appears that conventional route to K-doped materials leads to the materials with slow regeneration step, depending on the inherently slow diffusion through a solid matrix. However, the new soft-chemistry route to the high surface area undoped materials results in the much faster rates of reaction/regeneration. This is particularly significant for the design of the potential CO_2 capture processes based on lithium zirconates. The low temperature uptake of CO_2 has been studied in detail and the mechanism involving both reaction and chemisorption on native basic sites is proposed. The presence of significant low temperature uptake must be taken into account in detailed characterisation of these materials through extended thermal treatment of the 'as-received' samples in a CO_2 free environment. This may also lead to potential new applications involving medium range temperatures. Detailed thermodynamic analysis of the reactions confirmed feasibility of the low temperature reaction. Finally, the rate of reaction of CO_2 with Li_2ZrO_3 was found to be controlled by mass transfer at CO_2 pressures below 400 mbar.

Acknowledgements

Funding for the project was provided by EPSRC (from a ring-fenced fund allocated to Crystal Faraday Partnership, now part of the Chemistry Innovation Knowledge Transfer Network, UK) via grant GR/S24992/01 and MEL Chemicals. Samples of lithium zirconates from MEL Chemicals are greatly appreciated. In situ XRD measurements were performed at UOP by Jason Davis. This project was part of the joint research project involving Imperial College London (Drs. Esat Alpay and Frantisek Stepanek) and University of Leeds (Dr. Yulong Ding). Alina Iwan is grateful to the University of Bath for continuation of PhD studentship funding.

References

[1] R. Shinnar, The hydrogen economy, fuel cells and electric cars, Technol. Soc. 25 (2003) 455.
[2] J.C. Abanades, E.S. Rubin, E.J. Anthony, Sorbent cost and performance in CO_2 capture systems, Ind. Eng. Chem. Res. 43 (2004) 3462.
[3] J.R. Hufton, S. Mayorga, S. Sircar, Sorption-enhanced reaction process for hydrogen production, AIChE J. 45 (1999) 248.
[4] J. Hufton, W. Waldron, S. Weigel, M. Rao, S. Nataraj, S. Sircar, Sorption enhanced reaction process (SERP) for the production of hydrogen, in: Proceedings of the 2000 US DOE Hydrogen Program Review, 2000.
[5] G.C. Koumpouras, E. Alpay, F. Stepanek, Mathematical modelling of low-temperature hydrogen production with in situ CO_2 capture, Chem. Eng. Sci. 62 (2007) 2833.
[6] B. Balasubramanian, A.L. Ortiz, S. Kayatakoglu, D.P. Harris, Hydrogen from methane in a single-step process, Chem. Eng. Sci. 54 (1999) 3543.
[7] Z. Yong, V. Mata, A.E. Rodrigues, Adsorption of carbon dioxide at high temperature—a review, Sep. Purif. Technol. 26 (2002) 195.
[8] Y. Ding, E. Alpay, Equilibria and kinetics of CO_2 adsorption on hydrotalcite adsorbent, Chem. Eng. Sci. 55 (2000) 3461.
[9] H.T.J. Reijers, S.E.A. Valster-Schiermeier, P.D. Cobden, R.W.V.D. Brink, Hydrotalcite as CO_2 sorbent for sorption-enhanced steam reforming of methane, Ind. Eng. Chem. Res. 45 (2006) 2522.
[10] Z. Yong, V. Mata, A.E. Rodrigues, Adsorption of carbon dioxide onto hydrotalcite-like compounds (HTlcs) at high temperatures, Ind. Eng. Chem. Res. 40 (2001) 204.
[11] A. Ortiz, D. Harrison, Hydrogen production using sorption-enhanced reaction, Ind. Eng. Chem. Res. 40 (2001) 5102.
[12] K. Johnsen, H.J. Ryu, J.R. Grace, C.J. Lim, Sorption-enhanced steam reforming of methane in a fluidized bed reactor with dolomite as CO_2-acceptor, Chem. Eng. Sci. 61 (2006) 1195.
[13] K. Nakagawa, T. Ohashi, A novel method of CO_2 capture from high temperature gases, J. Electrochem. Soc. 145 (1998) 1344.
[14] R. Xiong, J. Ida, Y. Lin, Kinetics of carbon dioxide sorption on potassium-doped lithium zirconate, Chem. Eng. Sci. 58 (2003) 4377.
[15] E. Ochoa-Fernandez, H.K. Rusten, H.A. Jakobsen, M. Rønning, A. Holmen, D. Chen, Sorption enhanced hydrogen production by steam methane reforming using Li_2ZrO_3 as sorbent: sorption kinetics and reactor simulation, Catal. Today 106 (2005) 41.
[16] B.N. Nair, T. Yamaguchi, H. Kawamura, S.-I. Nakao, Processing of lithium zirconate for applications in carbon dioxide separation: structure and properties of the powders, J. Am. Ceram. Soc. 87 (2004) 68.
[17] M. Kato, K. Nakagawa, New series of lithium containing complex oxides, lithium silicates, for application as a high temperature CO_2 absorbent, J. Ceram. Soc. Jpn. 109 (2001) 911.
[18] C. Gauer, W. Heschel, Doped lithium orthosilicate for absorption of carbon dioxide, J. Mater. Sci. 41 (2006) 2405.
[19] M. Kato, S. Yoshikawa, K. Nakagawa, Carbon dioxide absorption by lithium orthosilicate in a wide range of temperature and carbon dioxide concentrations, J. Mater. Sci. Lett. 21 (2002) 485.
[20] J.-I. Ida, Y.S. Lin, Mechanism of high-temperature CO_2 sorption on lithium zirconate, Environ. Sci. Technol. 37 (2003) 1999.
[21] K. Essaki, K. Nakagawa, M. Kato, Acceleration effect of ternary carbonate on CO_2 absorption rate in lithium zirconate powder, J. Ceram. Soc. Jpn. 109 (2001) 829.
[22] K. Nakagawa, T. Ohashi, A reversible change between lithium zirconate and zirconia in molten carbonate, Electrochemistry 67 (1999) 618.
[23] J. Ida, R. Xiong, Y.S. Lin, Synthesis and CO_2 sorption properties of pure and modified lithium zirconate, Sep. Purif. Technol. 36 (2004) 41.
[24] D.J. Fauth, E.A. Frommell, J.S. Hoffman, R.P. Reasbeck, H.W. Pennline, Eutectic salt promoted lithium zirconate: novel high temperature sorbent for CO_2 capture, Fuel Process. Technol. 86 (2005) 1503.
[25] Y.-J. Wang, L. Qi, X.-Y. Wang, The study of Li_2ZrO_3 used for absorption of CO_2 at high temperature, Chin. J. Inorg. Chem. 19 (2003) 531.
[26] E. Ochoa-Fernandez, M. Ronning, T. Grande, D. Chen, Nanocrystalline lithium zirconate with improved kinetics for high-temperature CO_2 capture, Chem. Mater. 18 (2006) 1383.
[27] R. Xiong, J. Ida, Y.S. Lin, Kinetics of carbon dioxide sorption on potassium-doped lithium zirconate, Chem. Eng. Sci. 58 (2003) 4377.
[28] H. Stephenson, Lithium zirconate process, WO 2007/023294 A2 (2007).
[29] A. West, University of Aberdeen, Old Aberdeen, Scotland, ICDD Grant-in-Aid (1990).
[30] M. Yashima, T. Mitsuhashi, H. Takashina, M. Kakihana, T. Ikegami, M. Yoshimura, Tetragonal-monoclinic phase-transition enthalpy and temperature of ZrO_2–CeO_2 solid-solutions, J. Am. Ceram. Soc. 78 (1995) 2225.
[31] K. Essaki, K. Nakagawa, M. Kato, H. Uemoto, CO_2 absorption by lithium silicate at room temperature J, Chem. Eng. Jpn. 37 (2004) 772.
[32] M.W. Chase Jr., NIST-JANAF Thermochemical Tables, fourth edition, J. Phys. Chem. Ref. Data Monograph 9 (1998) 1.
[33] E.H.P. Cordfunke, R.R. Van Der Laan, G.P. Wyers, J.C. Van Miltenburg, The heat capacities and derived thermophysical properties of Li_2ZrO_3 and Li_8ZrO_6 at temperatures from 0 to 1000 K, J. Chem. Thermodyn. 24 (1992) 1251.
[34] P. Atkins, J. de Paula, Physical Chemistry, Oxford University Press, 2006.
[35] B.N. Nair, T. Yamaguchi, H. Kawamura, S. Nakao, Processing of lithium zirconate for applications in carbon dioxide separation: structure and properties of the powders, J. Am. Ceram. Soc. 87 (2004) 68.
[36] Y.-J. Wang, L. Qi, The influencing factor for CO_2 absorption of Li_2ZrO_3 at high temperature, Acta Phys.-Chim. Sin. 20 (2004) 364.
[37] H.A. Mosqueda, C. Vasquez, P. Bosch, H. Pfeiffer, Chemical sorption of carbon dioxide (CO_2) on lithium oxide (Li_2O), Chem. Mater. 18 (2006) 2307–2310.
[38] H. Pfeiffer, C. Vazquez, V.H. Lara, P. Bosch, Thermal behaviour and CO_2 adsorption of $Li_{2-x}Na_xZrO_3$ solid solutions, Chem. Mater. 19 (2007) 922–926.